International Journal of Computer Information Systems and Industrial Management Applications
ISSN 2150-7988 Volume 18(2026) pp. 1-18

https://doi.org/10.70917/ijcisim-2026-0170
Article

Research on Spatial Geometric Transformation and Path Planning Problems in Plant Landscape Design Based on Topology Optimization Algorithm

Hanhan Zhou [1,2,*] and Peiyun Bie [1]

[1] College of Tourism and landscape Architecture, Guilin University of Technology, Guilin 541004, Guangxi, China
[2] Institute of Guangxi Tourism Industry, Guilin 541004, Guangxi, China; ilyyyxx0118@163.com

Abstract: This paper designs the overall architecture and operational workflow of the system based on the hardware design of traditional digital plant landscape planning systems. Considering the system's flexibility, network operation mode, and operational security, the system's topological structure is determined. The system database is established from two aspects: data relationships and data types. This enables the system to perform digital plant landscape planning functions. On one hand, the system can achieve spatial geometric transformations of plant landscapes; on the other hand, it can optimize landscape paths based on an improved fish swarm algorithm. The landscape association values, minimum ecological damage values, and maximum spatial utilization values obtained from the plant landscape spatial element layout optimization model are superior to the target values of the actual scheme. Compared with the hybrid genetic algorithm, the path planning method based on the improved artificial fish school algorithm reduces the runtime by 34.4% and achieves better optimal solutions, path lengths, and smoothness than the hybrid genetic algorithm. This system can effectively solve the problems of spatial geometric transformation and path planning in plant landscape design.

Keywords: topological structure; spatial geometric transformation; artificial fish school algorithm; plant landscape design

1. Introduction

Landscape architecture is a field that combines art and science, with the goal of creating beautiful, practical, and sustainable landscape spaces that blend with the natural environment [1]. However, in the actual process of plant landscape design, designers often face multiple challenges. On the one hand, due to the diversity of plant species and the different flowering periods, ecological habits, colors, textures, and other attributes of different plants, it is difficult to systematically summarize the rules of plant combination, resulting in a high degree of difficulty in plant landscape design [2-4]. On the other hand, plant landscape design places high demands on designers, who must be familiar with a wide variety of plants and possess a high level of aesthetic sensibility in terms of color and texture coordination. However, there is a shortage of designers to meet the growing demand for plant design [5-8]. Additionally, since plant patches and combinations in plant landscapes interact with one another, even minor changes can have far-reaching consequences, making revisions to plant design plans time-consuming [9–11]. Furthermore, the creation of planting construction drawings involves a large amount of repetitive mechanical work, such as outlining, which significantly impacts work efficiency [12–13]. As the demand for plant landscape design continues to grow, the limitations of traditional design methods have become increasingly evident, making the optimization of plant landscape design methods particularly urgent [14-15].

With the rapid advancement of technology, new technologies such as digital technology, VR

technology, AR technology, drone remote sensing technology, big data intelligent algorithms, and computer-aided technology are increasingly being applied to plant landscape design. Deng, Y., et al. optimized the landscape design of digital cities based on spatial information technology, comprehensively considering residents' demand for green plants and the ecological value of urban spatial landscapes, striving to generate plant landscape design solutions that align with the interests of multiple stakeholders [16]. Pei, L. utilized virtual reality technology and embedded networks to expand the scope of urban plant landscape design methods, enabling designers to fully unleash their creativity while also facilitating the successful integration of diverse elements in landscape design, thereby enhancing the user experience [17]. Lin, X. et al. demonstrated that with the support of augmented reality technology, designers can preview design outcomes in real time, conduct data analysis, and optimize designs, thereby further enhancing the quality of landscape design [18]. Yang, D. and Huang, X. developed the Multi-Dense Network (MP-DenseNet) model based on DenseNet, which analyzes remote sensing data including vegetation cover classification to support the rational planning and design of plant protection landscapes [19]. Huang, L. investigated the application of big data technology in improving garden plant landscaping methods, and designed a landscape design indicator system suitable for commercial buildings targeting landscape professionals, demonstrating higher standardization and scientific rigor compared to traditional landscape design methods [20]. Du, J. addressed the issues of low plant diversity indices and landscape spatial pattern utilization rates in traditional landscape design methods by proposing the use of AutoCAD-assisted intelligent technology to visually reconstruct terrain, planning, and planting design content, providing valuable references for designers [21]. The aforementioned methods offer solutions and insights to address the limitations of traditional design methods, enhancing the scientific rigor and precision of design, thereby transforming design concepts and methodologies. This supports the intelligent, personalized, and sustainable development of plant landscape design.

The digital plant landscape planning system designed in this paper determines the system network topology based on the architecture. When the system undergoes geometric changes in the landscape space, it constructs a set of texture feature vectors along the edges of the spatial element layout images to extract spatial element layout features. Based on this, it establishes a factor system for optimizing element layout. Using the information weight and value weight of evaluation indicators, it constructs a spatial element layout optimization model to achieve spatial geometric transformation. When optimizing landscape paths, the system incorporates the harmonic search algorithm into the artificial fish school algorithm, applying subtle perturbations to the fish school information to obtain a more optimal global optimal path. Taking Z Park as an example, the system designed in this paper is applied to achieve spatial geometric transformations of the landscape and optimization of garden paths.

2. Construction of a Plant Landscape Design Planning System

2.1. Overall System Architecture

The digital plant landscape planning system designed in this paper will be developed based on the hardware design of traditional digital plant landscape planning systems, with a focus on designing the software for the digital plant landscape planning system. The system takes into account the requirements for digital plant landscape planning, as well as principles such as practicality, advanced functionality, security and reliability, openness and sharing, cost-effectiveness, and ease of implementation.

The system's overall architecture is divided into three layers: the data service layer, the spatial data engine and visualization technology layer, and the application client layer. The application client layer is used to display system applications, with the office module in the service layer providing services to the client, offering users the required digital plant landscape spatial and non-spatial data. Users can use the digital plant landscape configuration tool to plan digital plant landscapes based on the spatial and non-spatial data, utilizing visualization technology to create a visual digital plant landscape model. The database parameter configuration tool module connects to the data service layer. Each time the office module is used, the database parameter configuration tool module performs parameter configuration and connects to the database parameter file. The system maintenance module ensures system operation and manages system business and data, including three units: personnel business management, map management, and tool management. The office module serves as the user's digital plant landscape planning operation layer, including case handling units (case reception and office columns), map operations, map management, and tool units.

The database engine serves as the system's middle layer. The ArcSDE database engine retrieves spatial and non-spatial data from the data service layer and can also store spatial and non-spatial data required for digital plant landscape planning. Its programming interface enhances the data service layer's access rate while minimizing system memory and disk space usage. Visualization technology is used to give the system data an outer contour and specific appearance, such as trees, buildings, etc.

2.2. Determining the System Topology

The system must have a flexible and convenient network operation mode that can process system data in a timely manner, filter data information that threatens the system, prevent external intrusions, and ensure the security of system operation. The system topology structure determined by the digital plant landscape planning system designed in this paper is shown in Figure 1.

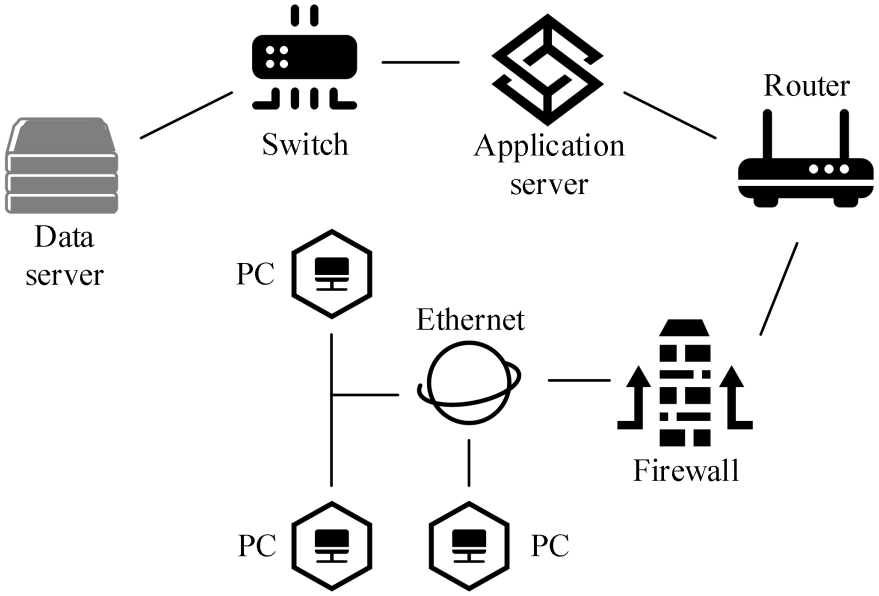

Figure 1. System topology.

2.3. Establish a System Database

The established system database takes into account the existence of visual data in digital plant landscape data, which places high demands on the database during the data adjustment process. Based on the five principles of database security, sharing, independence, efficiency, and scalability, the Oracle 9i database, which is of a higher level and operates at a faster speed, was selected as the system database for this project.

Additionally, in practical applications, digital plant landscape data will continue to grow. Therefore, it is necessary to consider the data access rate of the database. This requires archiving the data within the database to establish a database management model where database tables and database archives coexist, thereby reducing the amount of data in the database cache and improving the response efficiency of database data during data queries. When users query data, they should not rely solely on query conditions to retrieve data information from the database, as this would impair user data query efficiency. Therefore, in the database established in this study, database indexes are designed to enhance the inherent characteristics of the database server. Based on the three components of digital plant landscape data—entities, attributes, and relationships—the database E-R diagram is shown in Figure 2. In the diagram, M and N represent different types of relationships, where 1:1 denotes a one-to-one relationship, 1:N denotes a one-to-many relationship, and M:N denotes a many-to-many relationship. The system database E-R diagram divides the data into four parts: user information, administrators, construction drawings, and construction drawing classifications. It stores the digital plant landscape data that users are currently planning or have already completed, i.e., the non-spatial data in the database. In addition, the system database also includes the spatial data of the digital plant landscape planning.

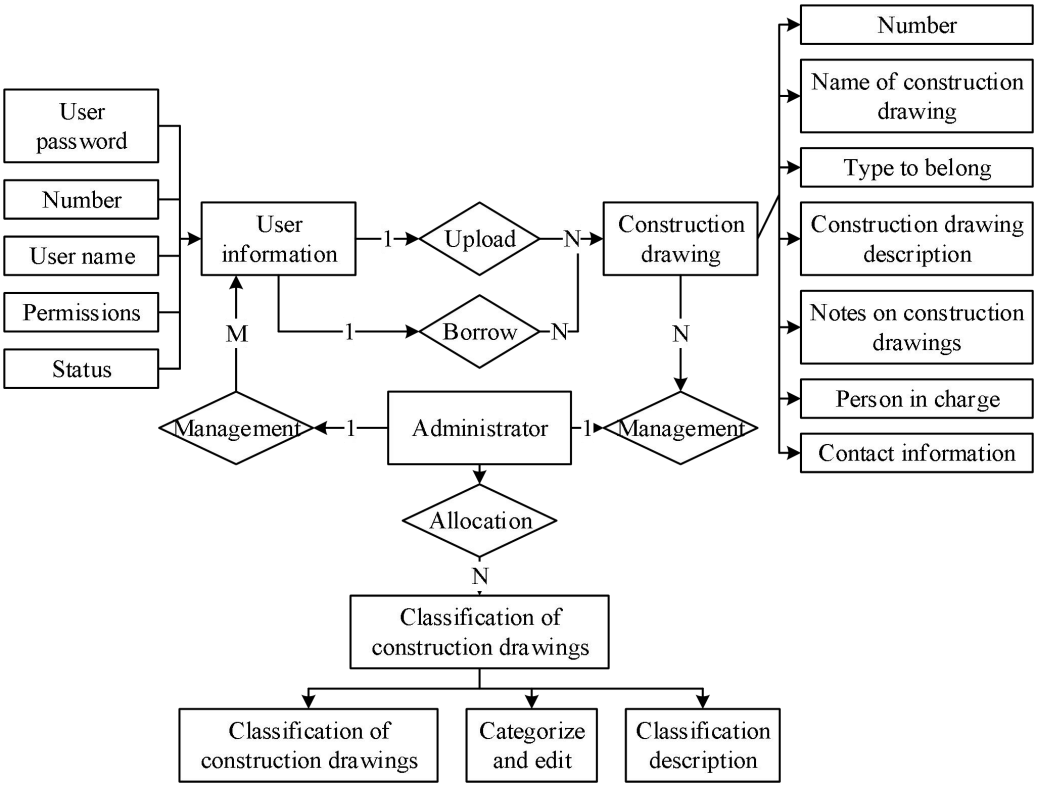

Figure 2. Database E-R.

2.4. Planning Digital Plant Landscapes

The system architecture of the digital plant landscape planning system design employs visualization technology, and the digital plant landscape planning is implemented using a parametric approach. The digital plant landscape planning process involves analyzing the plant landscape site to identify both quantifiable and non-quantifiable factors, and storing data for both types of factors in the system database. Through the system's office module, a quantitative data algorithm for the digital plant landscape is generated, and plant landscape graphics are output. Using visualization technology and plant landscape graphics, a digital plant landscape model is constructed to complete the digital plant landscape planning. At this point, the planned digital plant landscape can be subjected to further construction, management, and maintenance.

3. Spatial Geometric Transformation and Path Planning Design Methods

3.1. Building a Plant Landscape Spatial Layout Planning Model

3.1.1. Extracting Landscape Spatial Element Layout Characteristics

In order to improve the environmental quality of the landscape, the layout images of landscape spatial elements are normalized to remove the DC component of the layout images, i.e.,:

$$G(x,y) = R^{-(x^2+y^2)} \tag{1}$$

In the formula: x and y represent the horizontal and vertical coordinates of the spatial element layout, and R represents the normalization factor.

After normalization, the edges of the spatial element layout image can be extracted. By sorting the image resolution, the spatial element layout image is decomposed into subbands in different directions, and the calculation formula is:

$$r_n = \frac{G(x,y)}{\varepsilon_n^2} \tag{2}$$

In the formula: ε_n^2 represents the variance of the subband of the spatial element layout image

decomposition, and n represents the level of image decomposition.

At different decomposition levels, the subbands of the spatial element layout image are calculated with weights to obtain a weighted undirected graph of the landscape spatial element layout, represented as:

$$g = (a, b, d) \tag{3}$$

In the formula, a, b , and d represent the vertices of the three decomposition subbands of the weighted undirected graph, respectively.

The weighted undirected graph in formula (3) is used as a constraint in the single-parent genetic algorithm [22] to decompose the spatial element layout image layer and calculate the energy of the wavelet coefficients. Considering that the energy of the wavelet coefficients at the edges of the image remains unchanged when the spatial element layout image is rotated under the same texture, the energy of the wavelet coefficients at the edges of the spatial element layout image is calculated by accumulating the variance of the decomposed subbands, i.e.,:

$$\chi_i = \sum_{j=1}^{3} \kappa_{i,j} \tag{4}$$

In the formula: $\kappa_{i,j}$ represents the sum of the wavelet coefficient energies obtained from the edge of the spatial element layout image in the $j(\leq 3)$ direction at the i layer. Since the three decomposition subbands of the weighted undirected graph each contain three vertices, the direction of division according to the number of subband layers must be less than or equal to three.

After the texture of the spatial element layout image is rotated, at the same decomposition level, the subband coefficient with the strongest energy in a certain direction may appear in another subband, but the magnitude of the energy will not change. In this case, the following situation may occur:

$$v_i = \max(\kappa_{i,j}) \tag{5}$$

In the formula: v_i represents the final large energy value of the spatial element layout image edge decomposition coefficient.

Based on the decomposition level of the image, construct a set of texture feature vectors for the spatial element layout image edge, extract the spatial element layout features of the landscape, and represent them as:

$$Z = [X_1, X_2, X_3, X_4, v_1, v_2, v_3, v_4] \tag{6}$$

By normalizing the layout images of landscape spatial elements, the images are decomposed into subbands in different directions, thereby obtaining a weighted undirected graph of the layout of landscape spatial elements. Based on the energy sum of the edge wavelet coefficients of the spatial element layout images, the spatial element layout features of the landscape are extracted.

3.1.2. Building a Landscape Spatial Element Layout Optimization Model

Based on the layout characteristics of landscape spatial elements, define the rationality factors of landscape spatial element layout and quantify them, namely:

$$Lt(u) = \frac{\ell(u) \times \Omega}{\eta \cdot X \cdot Z} + k^* \tag{7}$$

In the formula: $\ell(u)$ represents the coordination of spatial element u , Ω represents the sample set of rationality indicators for spatial element layout, η represents the partial regression coefficient of spatial elements, X represents the display representation of spatial element layout, and k^* represents the response mechanism of spatial element layout.

Based on the quantification results, a factor system for optimizing the layout of landscape spatial elements is constructed, and the weights of each evaluation factor are calculated, i.e.,:

$$\omega = \frac{E \times \delta}{Z} + p \times L(u) \tag{8}$$

In the formula: E represents the spatial element layout rationality evaluation factor, δ represents the number of rationality evaluation indicators, and p represents the expert evaluation results for spatial

element layout rationality.

Using the weighted sum method, the weights of the spatial element layout rationality evaluation indicators are divided into information weight and value weight, namely:

$$\tilde{\omega} = \frac{\sigma \times \vartheta}{h_{op}} \times K_{op} \tag{9}$$

In the formula: σ and ϑ represent the multi-scale characteristics and static evaluation values of the rationality of spatial element layout, while h_{op} and K_{op} represent the evaluation value and evaluation grade of the o th expert for the rationality of the p th spatial element layout.

Using the information weight and value weight in the evaluation of the rationality of landscape spatial element layout, a weight matrix for the spatial element layout optimization index is constructed, expressed as:

$$W = \frac{\varepsilon \times S}{\tilde{\omega} \times \Lambda^{\delta}} \times \mu_{\max} \times \psi \tag{10}$$

In the formula: ε represents the independent variable of spatial element layout optimization, S represents the dynamic spatiotemporal nature of spatial element distribution in the landscape, Λ^{δ} represents the reasonable range of spatial element layout optimization, $\mu_{\max}$ represents the maximum difference of spatial element layout optimization indicators, and ψ represents the value of the optimization decision variable.

Based on the weight matrix of the spatial element layout optimization indicators, a landscape spatial element layout optimization model is constructed, namely:

$$\Phi = \frac{\omega^{*} \times \omega}{W} \times Lt(u) \tag{11}$$

In the formula: ω^{*} represents the ranking results of the weighting of spatial element layout optimization indicators.

Based on the above process, a weighting matrix for spatial element layout optimization indicators is established to construct a landscape spatial element layout optimization model.

3.2. Plant Landscape Path Planning Based on an Improved Artificial Fish School Algorithm

3.2.1. Path Planning Model

Path planning involves constructing an optimal tour path based on the user's current location and destination. This paper formulates the problem as finding the optimal path from the starting point $St(x_s, y_s)$ to the target point $Tt(x_\tau, y_\tau)$ in a given rectangular coordinate system xOy. To simplify calculations, this paper performs an affine transformation on the Cartesian coordinate system, representing the path between the starting point and the destination point as a line segment ST. Then, any point $P(X,Y)$ in the xOy coordinate system can be expressed as:

$$\begin{bmatrix} x \\ y \end{bmatrix} = \begin{bmatrix} \cos\theta & -\sin\theta \\ \sin\theta & \cos\theta \end{bmatrix}^{-1} \cdot \left(\begin{bmatrix} X \\ Y \end{bmatrix} - \begin{bmatrix} x_s \\ y_s \end{bmatrix} \right) \tag{12}$$

$$\theta = \arcsin \frac{y_T - y_S}{|ST|} \tag{13}$$

In the equation: θ is the distance between the line segment ST and the x-axis. (x, y) is the coordinate point after the mapping of $P(X,Y)$.

Since there are various obstacles in path planning, in order to avoid collisions between the guidance path and obstacles, the following collision avoidance conditions are defined in this paper.

(a) Polygon collision avoidance. To prevent the planned path from colliding with polygon obstacles, the condition set in this paper is:

$$\begin{aligned}&[(P_1-Q_1)(Q_2-Q_1)]\cdot[(Q_2-Q_1)(P_2-P_1)]>0\\&[(Q_1-P_1)(P_2-P_1)]\cdot[(Q_2-P_1)(P_2-P_1)]>0\end{aligned}\tag{14}$$

In the formula, the endpoints of the two line segments are represented by P_2P_1, Q_2Q_1.

(b) Preventing collisions with circular obstacles. In order to prevent the planned path from colliding with circular obstacles, the conditions set in this paper are:

$$\frac{t\,|\,t(y_2-y_1)x_0-t(x_2-x_1)y_0+t(y_1x_2-x_1y_2)\,|}{\sqrt{(y_2-y_1)^2+(x_2-x_1)^2}}>R\tag{15}$$

In the formula: x_2x_1, y_2y_1 are the endpoints of the two line segments. (x_0, y_0) is the center of the circular obstacle. R is the radius.

3.2.2. Path Planning Based on Improved Artificial Fish School Algorithm

In order to obtain a shorter and smoother target route, this paper combines the weight coefficient method to define the guidance path. The objective function includes the total length $f_1(P)$ and smoothness $f_2(P)$ objectives, which are specifically expressed as follows:

$$f(P)=w_1f_1(P)+w_2f_2(P)\tag{16}$$

In the equation, w_1, w_2 are weight coefficients.

The article uses the fish school algorithm to solve the above multi-objective optimization problem, which is an intelligent optimization algorithm derived from bionics. By using computer programs to simulate the feeding, grouping, tailing, and random behavior of fish schools, the objective function is solved and its optimal solution is obtained [23]. However, this algorithm is prone to blind search in the early stages. To enhance the algorithm's global search capability, this paper introduces the harmonic search algorithm [24]. By generating a large number of local optimal solutions during the iteration process, the search efficiency of the fish swarm's random behavior is improved.

In this paper, it is assumed that there are N artificial fish in the search space, and $X=(x_1,x_2,\cdots,x_D)$ represents the state information of the artificial fish, $ft(x)$ denotes food concentration, Y represents the fitness function value shown in Equation (16), and $|X_i-X_j|$ denotes the distance between artificial fish i and j. The paper assigns the adjusted artificial fish state values from the harmonic search algorithm to the artificial fish swarm, as shown in the following formula:

$$X=(x_1,x_2,\cdots,x_D)=X_i=(x_{i1},x_{i2},\cdots,x_{iD})\tag{17}$$

Randomly select a state X_j from the visual field of artificial fish X_i to update X_i, as shown in the following formula:

$$X_j=X_i+Visual\cdot Rand()\tag{18}$$

When the updated state X_i is better than X_j, move to state X_j by a certain step size, as shown in the following formula:

$$X_i^{t+1}=X_i^t+\frac{X_i-X_i^t}{t\,\|\,X_i-X_i^t\,\|}\cdot step\cdot Rand()\tag{19}$$

When state X_i is not better than X_j, continue updating X_j until the maximum foraging count is reached, as shown in the following formula:

$$X_i^{t+1}=x_i^t+Visual\cdot Rand()\tag{20}$$

Assume that the state of an artificial fish is X_i, and within its field of vision $d_{ij}<Visual$, the number of other artificial fish is n_i, then the center position of these n_i artificial fish is X_c. When

$Y_c / n_i > Y_i$, the density of artificial fish at this position is lower than the food density, so X_i moves one step forward toward state X_c according to equation (10). Otherwise, continue foraging:

$$X_i^{t+1} = X_i^t + \frac{X_C - X_i^t}{t \| X_C - X_i^t \|} \cdot step \cdot Rand\ () \tag{21}$$

For artificial fish in state X_i, calculate the maximum fitness value Y_j of X_j by searching for the number of peers n_f around it. When $Y_j / n_f < Y_i$, the density of artificial fish at this position is higher than the food density, so it can move forward to state X_j according to equation (21). Otherwise, continue foraging:

$$X_i^{t+1} = X_i^t + \frac{X_j - X_i^t}{t \| X_j - X_i^t \|} \cdot step \cdot Rand\ () \tag{22}$$

Based on the above steps and optimization operations, this paper combines fish density and tailing behavior to form an artificial fish population, and generates a new population through optimization operations. Then, harmonic search algorithms are used for fine-tuning perturbations to quickly escape local optima and obtain global optima. Among them, the perturbation factor of harmonic search is $\delta_j(t)$, and the state evolution formula of artificial fish is:

$$x_i^{'}(j) = x_i(j) + \delta_j(t) \tag{23}$$

The overall process of the improved artificial fish swarm search algorithm proposed in this paper is shown in Figure 3.

(a) Algorithm initialization. Set the number of fish to N, the field of view of each fish to Visual, and the update step to Step.

(b) Fish behavior selection. Based on each fish's trailing behavior and foraging behavior, obtain the corresponding X_j, and perform chaotic search on each component of X_j according to $X_{new} = X_i + 2 \cdot Visual$. When the state X_i is better than X_j, update X_i using equation (21). Otherwise, update X_i using equation (22).

(c) Calculate the fitness function of the fish school using equation (16). When the fitness function meets the new conditions, it is referred to as the new population. Otherwise, return to step (a) to reinitialize the fish school.

(d) Use the harmonic search algorithm to perturb the fish swarm state according to equation (23), and compare the updated fitness values of the fish swarm. When the fitness value is better than the historical optimal value, update the fish swarm library.

(e) Determine whether the fitness function has reached the optimal value. If it has reached the optimal value, exit the calculation. Otherwise, return to step (d) to continue searching for a better fish swarm.

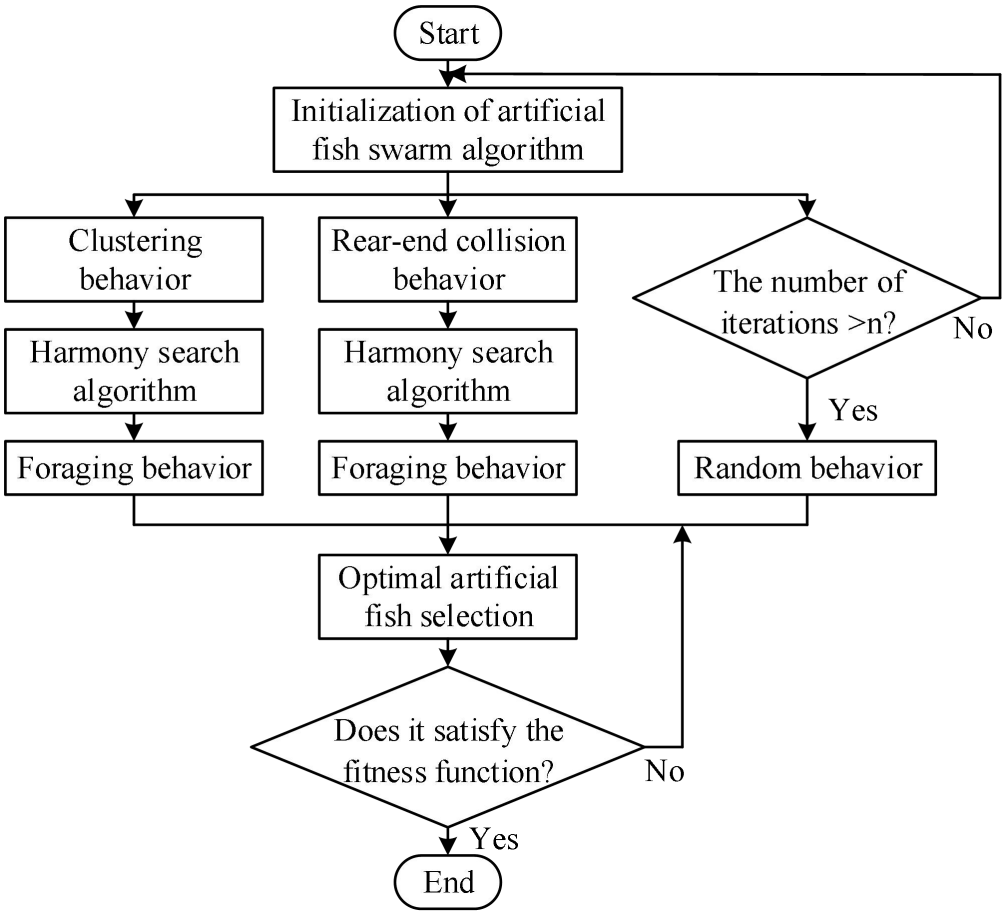

Figure 3. shows the process of the improved artificial fish swarm search algorithm.

4. Case Studies

Z Park is planned as a district-level park in a certain city, covering an area of 30 hectares. The landscape layout of the entire site primarily features a mountain-ringed, water-enclosed form. The central part of the park consists of an irregularly shaped water body spanning 15 hectares, with the terrain sloping from east to west. Currently, the plant landscape within the site is dominated by trees, with other ornamental plants scattered throughout the central activity area. The overall landscape layout of the park is disorganized, and the spatial relationships are chaotic. Therefore, it is necessary to enhance the integration of plant landscapes with the site and optimize the coordination of the park's landscape garden plant layout planning. Taking this park as an example, the spatial geometric transformation and path planning design methods described above are applied to its planning and design.

4.1. Analysis of the Spatial Sequence of Plant Landscapes in Parks

4.1.1. Feasibility Layer Analysis

(1) Maximum diameter of the feasible layer field of view

The maximum diameter of the feasible layer field of view reflects spatial depth. The changes in the maximum diameter of the feasible layer field of view are shown in Figure 4. The range of the maximum radius of the feasible layer field of view is between 19.63 and 201.52 m, with an average value of 96.32 m. The data exhibits significant variability, indicating that for the feasible layer space of the park, some feasible layers have greater depth, resulting in longer line-of-sight lengths at that point. Conversely, in areas with smaller feasible layer depths, the space is more convoluted, significantly obstructing the line of sight. When moving through the feasible layer space, the spatial depth at each viewpoint is small, causing the line of sight in the direction of travel to constantly change, evoking a sense of winding paths leading to secluded areas.

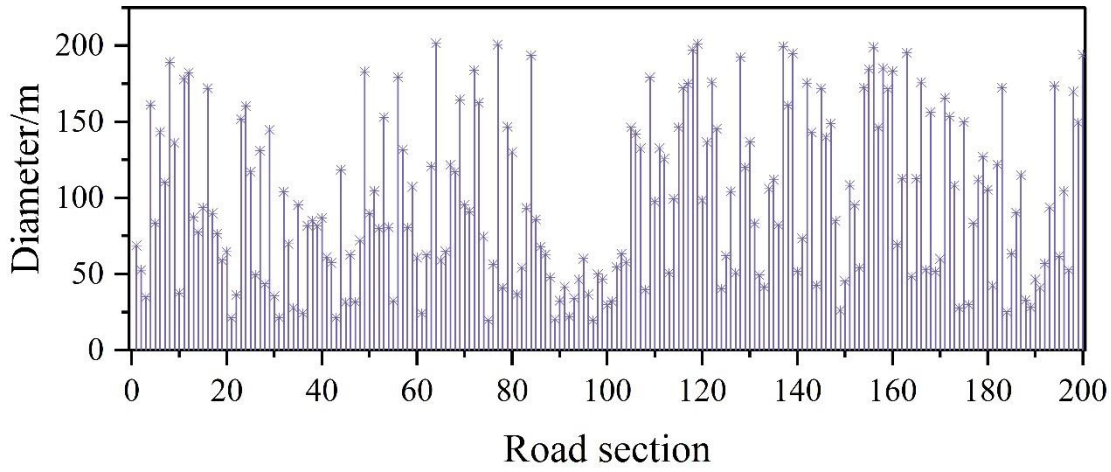

Figure 4. The maximum diameter of the feasible layer is changed.

(2) Minimum diameter of the feasible layer field of view

The minimum diameter of the feasible layer field of view can indirectly indicate the width of the feasible layer spatial entity. The variation in the minimum diameter of the feasible layer field of view is shown in Figure 5. The range of the minimum diameter of the feasible layer field of view is between 1.02 and 13.63 m, with an average value of 4.35 m. The minimum diameter of the feasible layer for most viewpoints is between 1.6 and 4 m, which is close to the width of the garden path along this tour route. This indicates that the activity space is relatively open.

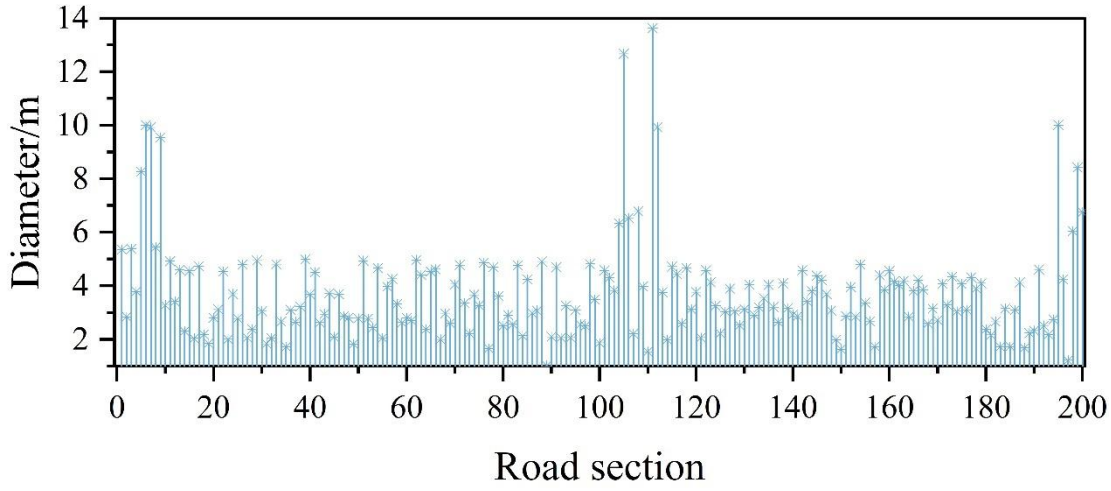

Figure 5. The minimum diameter of the horizon is changed.

(3) Feasible layer field of view area

The feasible layer field of view area reflects the perceived area of the physical space from that viewpoint. Changes in the feasible layer field of view area are shown in Figure 6. The field of view area of the feasible layer space ranges from 52.63 to 2952.63 m², with an average value of 863.65 m².

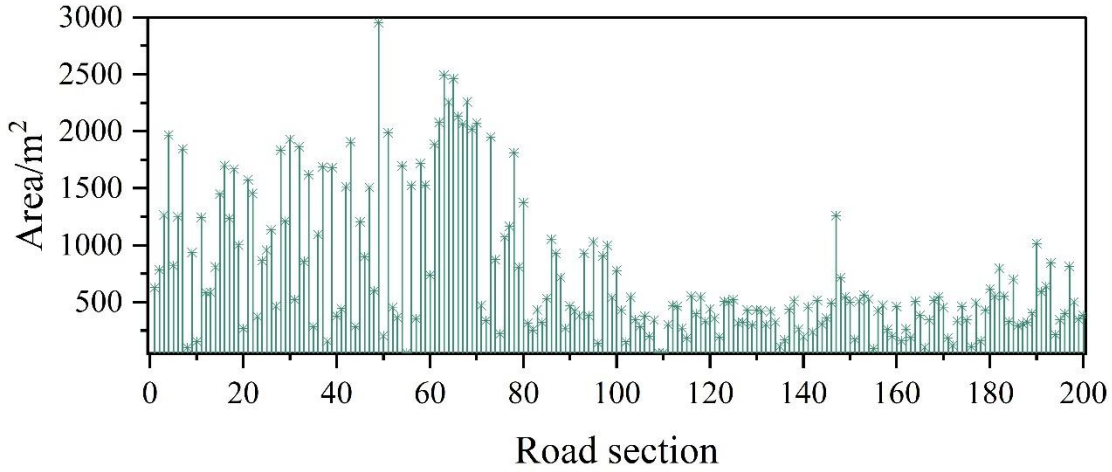

Figure 6. Feasible horizon area change.

4.1.2. Visual Layer Analysis

(1) Maximum diameter of the visible layer field of view

The maximum diameter of the visible layer field of view reflects the maximum viewing distance from that viewpoint. Changes in the maximum diameter of the visible layer field of view are shown in Figure 7. The maximum diameter of the visible layer viewpoint ranges from 20.03 to 496.35 m, with an average value of 207.63 m. The line chart exhibits strong fluctuations, and these fluctuations are more pronounced than those in the distribution chart of the maximum diameter of the feasible layer field of view. This indicates that the spatial depth changes and frequency of the park's visible layer are greater than those of the feasible layer.

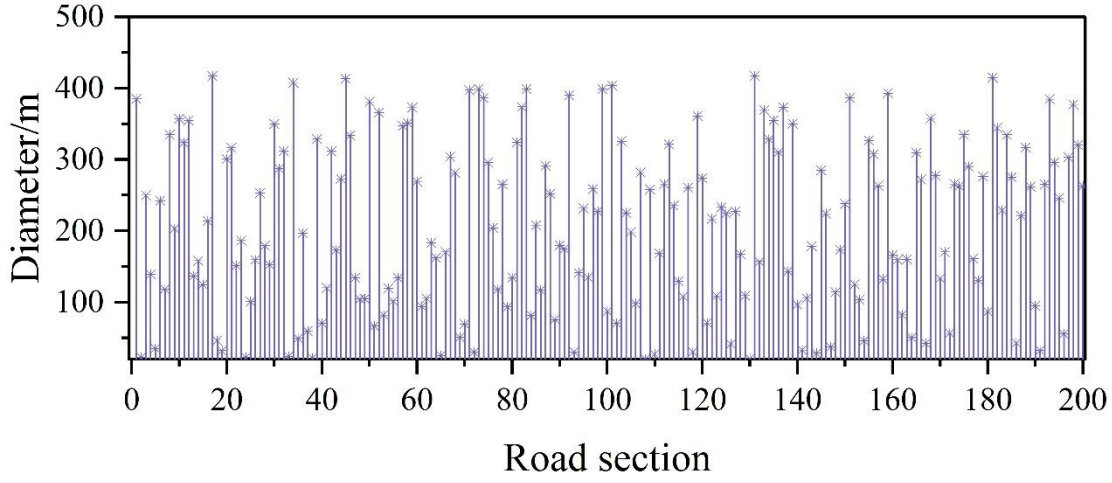

Figure 7. The maximum diameter of the visual horizon domain.

(2) Minimum diameter of the visible layer field of view

The minimum diameter of the visible layer field of view can, to a certain extent, reflect the visual center of the space. Changes in the minimum diameter of the visible layer field of view are shown in Figure 8. In the visible layer space, the distribution range of the minimum diameter of the viewpoint is between 0.46 and 14.1 m, with an average value of 4.59 m, which is not significantly different from the distribution of the minimum field of view diameter of the feasible layer.

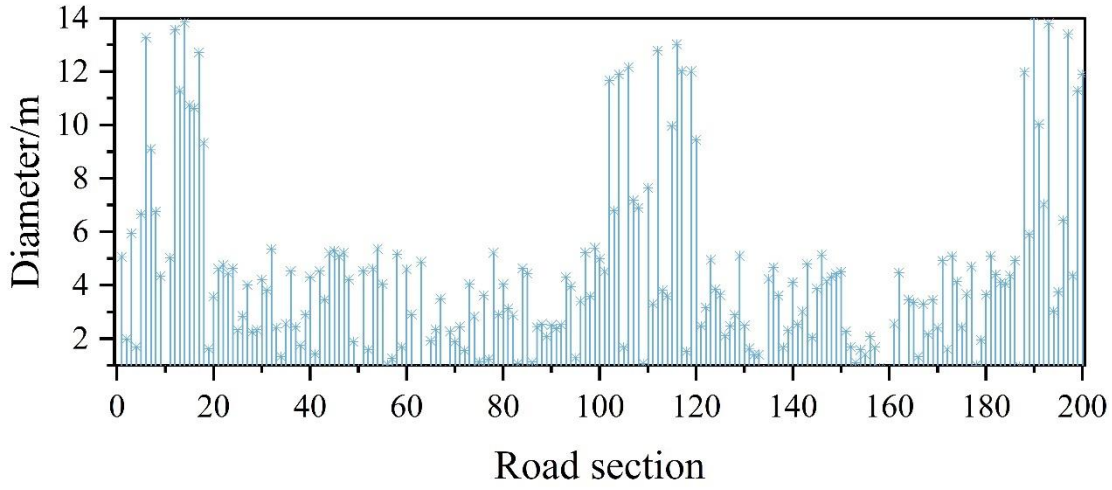

Figure 8. Visual horizon minimum diameter variation.

(3) Visible layer field of view area

The visible layer field of view area reflects the perceptible area of the visible layer space for visitors. The distribution of the visible layer field of view area is shown in Figure 9. The distribution range of the visible layer field of view area is between 306.52 and 13,635.6 m², with an average value of 4,563.96 m².

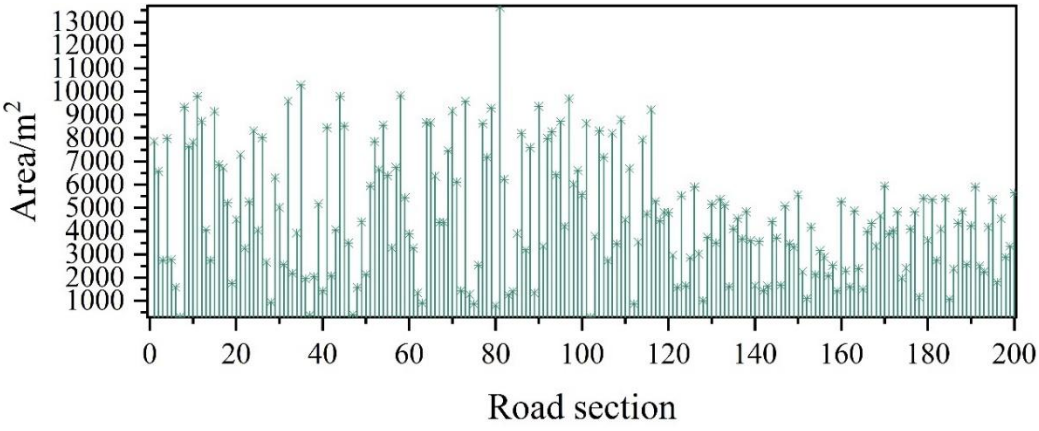

Figure 9. Visual horizon field.

4.1.3. Layout Characteristics of Landscape Space Elements

The spatial unit model classifies spaces into three types based on human spatial perception: enclosed spaces, semi-open spaces, and open spaces.

Enclosed spaces—both the visible space and the accessible space are small in scale, with the visual interface and spatial interface largely overlapping, resulting in strong spatial enclosure. The space exhibits a centripetal nature.

Semi-open space—The accessible space is small-scale, while the visible space is large-scale. The visual interface is larger than the spatial interface, resulting in a more open field of view.

Open space—Both the accessible space and the visible space are large-scale, with weak spatial enclosure.

(1) Results of spatial syntax research

By categorizing 200 viewpoints according to the above table, 11 landscape space types in Z Park were identified, as shown in Table 1. Among them, the view field classification results for “open space” include sections 4, 5, 6, 8, 10, and 11. “Semi-open space” corresponds to section 2, while “closed space” includes sections 1, 3, 7, and 9.

Table 1. Spatial type change.

Section	Apparent point	Space type
1	1~11	Enclosed space
2	12~19	Open in half space
3	20~40	Enclosed space
4	41~50	Open space
5	51~60	Open space
6	61~80	Open space
7	81~110	Enclosed space
8	111~145	Open space
9	146~159	Enclosed space
10	160~180	Open space
11	181~200	Open space

(2) Comparison of questionnaire survey data with spatial syntax research results

To verify the above results, a survey was conducted on the actual spatial perceptions of visitors along each road segment. Each evaluation criterion was scored on a scale of 1 to 5. Among the 230 questionnaires collected, each of the 11 road segments had at least 20 evaluations, and the average score was calculated. A score of 1 to 2.5 was classified as a closed space. When the score was between 2.5 and 3.5, it was classified as a semi-open space. When the score was between 3.5 and 5, it was classified as an open space.

The results of the visitor spatial perception questionnaire are shown in Table 2. It was found that in "Section 4," the visual field classification result was "open space," while the visitors' perceived result was "semi-open space." After on-site comparison and analysis, it was determined that the northern side of this section allows visitors to overlook Xili Lake through the grassy space north of the Zangshan Pavilion, but the south side is covered by trees, so visitors perceive it as a semi-open space, while the visual field classification categorizes it as an open space. Therefore, it was corrected to a semi-open space. After comparison, the consistency between the two evaluations exceeded 90%, indicating that classifying the plant landscape space types in Z Park based on visual field classification has certain significance.

Table 2. The spatial feeling of the visitor is the result of the questionnaire.

Section	Apparent point	Scoring	Space type
1	1~11	1.3	Enclosed space
2	12~19	2.9	Open in half space
3	20~40	4.6	Enclosed space
4	41~50	3.1	Open in half space
5	51~60	3.9	Open space
6	61~80	4.2	Open space
7	81~110	2.1	Enclosed space
8	111~145	4.4	Open space
9	146~159	2.2	Enclosed space
10	160~180	4.3	Open space
11	181~200	4.2	Open space

In summary, the layout characteristics of the entire landscape space elements are:

closed-semi-open-closed-semi-open-open-open-closed-open-closed-open-open.

4.2. Application Results of Plant Layout Planning Model

4.2.1. Model Application Results

Based on the results of spatial scale feature information extraction for landscape groups, it can be seen that the overall layout of the planning object extends from north to south. The primary objective of the park landscape plant layout planning is achieved through the planning of noise-reducing forests and tree group spaces, with plant landscape arrangements highlighting the key features of the layout planning.

Using the plant landscape spatial element layout optimization model designed in this paper, the constructed model is parameterized on the Rhinoceros+Grasshopper platform. The plant landscape layout of the study area is planned, and the generated plant spatial layout is shown in Figure 10. To ensure the overall quality of the planned plant landscape and maximize the park's aesthetic value, the main walking paths of the park are designated as the primary locations for plant landscape selection, serving as the main viewing points for the park's plant landscapes. Using an adult's average walking speed of approximately 0.62 meters as a reference, the locations of other viewing points are designed. Based on the standard that adults can clearly see plant landscape details within a 35–45-meter viewing range, corresponding distance points are randomly generated. Excluding cases where distance points are too close, the layout of tree groups and plant locations within the park is reasonably arranged to generate dense and sparse forests covering the entire park. Noise sources within and outside the park are fully considered, with noise-reducing forests established to meet the relevant requirements for Class I sound environments in parks. Combining vegetation shapes to construct plant landscapes, a sawtooth-shaped forest edge line plant landscape is formed to ensure the aesthetic effect of the main scenery.

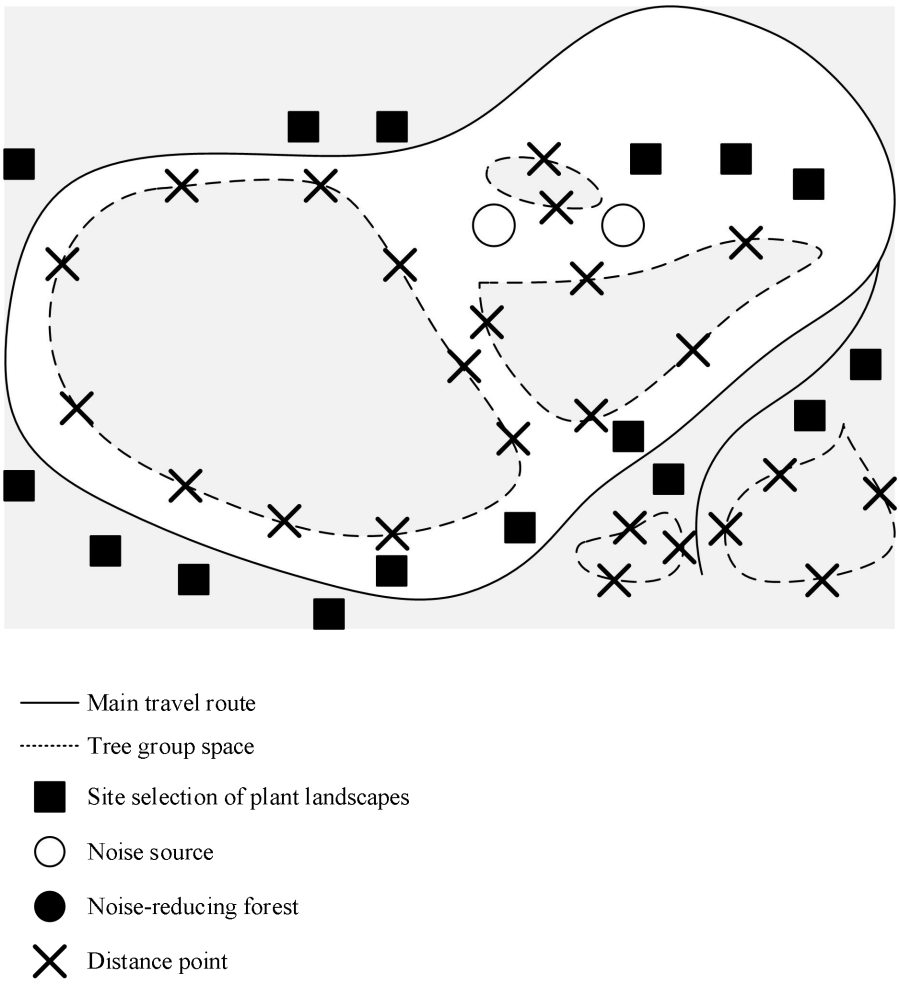

Figure 10. Plant space layout.

4.2.2. Experimental Analysis of Model Target Value Comparison

Select the feature-constrained plant layout planning model (Model 1) and the fuzzy dual-objective planning layout model (Model 2) as experimental comparison models. Under identical experimental conditions, run all three models simultaneously in the simulation software. The actual objective values 1, 2, and 3 correspond to the highest landscape association value, the minimum ecological damage value, and the maximum spatial utilization value in the actual park. By comparing the actual layout planning scheme with the layout schemes obtained from different models, the application performance of various planning models in landscape plant layout was evaluated. The model comparison results are shown in Table 3. It can be seen that, when compared with the actual layout planning scheme's target values, the landscape association relationship value, minimum ecological environment damage value, and maximum spatial utilization value obtained by the plant landscape spatial element layout optimization model constructed in this paper are all superior to the actual scheme's target values. Meanwhile, the target values obtained by Model 1 and Model 2 are both higher than the actual target values, indicating that the model constructed in this paper is feasible and effective for landscape garden plant layout planning.

Table 3. Model comparison results.

Layout plan	Target value one	Target value two	Target value three
Actual plan	8691	3.456	0.347
Model 1	110048	4.52	0.45
Model 2	28797	3.643	0.662
Ours	5091	1.089	0.228

*4.3. Application Results of Path Planni*ng Model

4.3.1. Experimental Parameters

To validate the effectiveness of the path planning method based on the improved artificial fish school algorithm, simulation experiments were conducted in the Matlab simulation environment. All experiments in this paper were conducted in the Matlab 2015b environment under the Windows 7 operating system, with an Intel® Core™ i5-3210M CPU@2.50 GHz processor and 8GB of memory. During the experiments in this paper, the maximum number of iterations was set to 2000.

4.3.2. Analysis of Simulation Results

The path planning method based on the hybrid genetic algorithm and the method proposed in this paper were each executed 10 times in a 100×100 simulation environment map. The simulation paths generated by the two methods in the map are shown in Figure 11. It can be seen that the path planned by the method proposed in this paper has fewer turning points and a shorter distance, clearly outperforming the hybrid genetic algorithm.

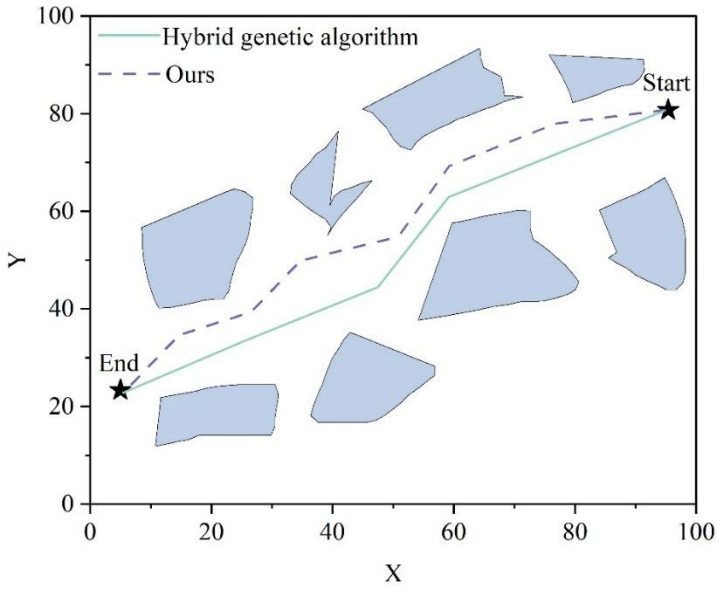

Figure 11. Two approaches to the simulation path in the map.

The iteration curves of the two methods are shown in Figure 12. It can be seen that, compared with the hybrid genetic algorithm, the method proposed in this paper can find the global optimal solution more quickly, reflecting the fast convergence performance of the improved artificial fish school algorithm.

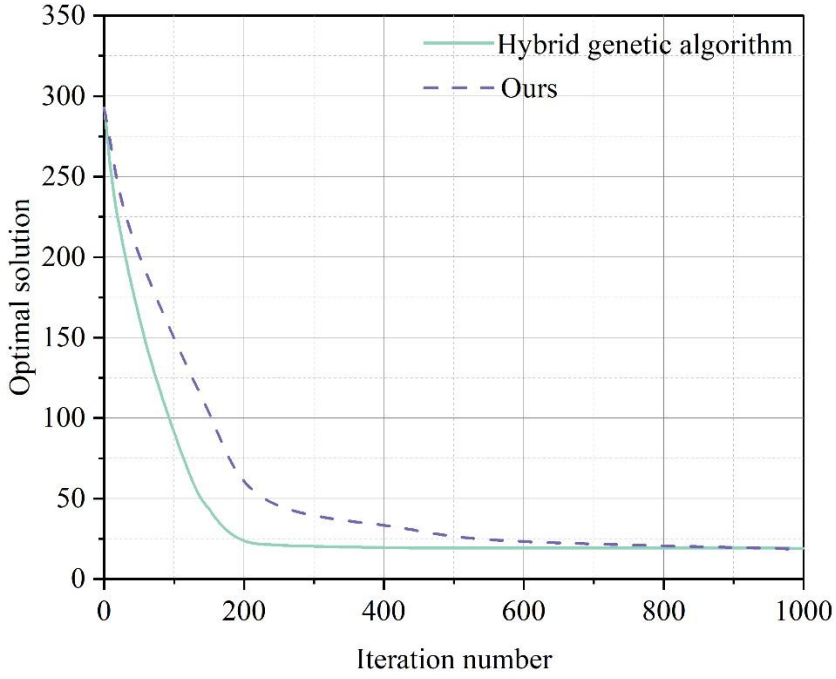

Figure 12. Two approaches to the iterative curves in the simulation map.

4.3.3. Analysis of Application Results

To validate the effectiveness of the proposed path planning method in addressing real-world scenarios, specific tests were conducted at Z Park.

The statistical results of path planning data for the two methods are shown in Table 4. The path planning method based on the artificial fish school algorithm reduced the running time by 34.4%, indicating that the improved algorithm reduced the number of iterations required, significantly improving path planning efficiency. From the comparison results of the optimal solution, path length, and smoothness, it can be seen that the method proposed in this paper performs better in terms of

convergence accuracy and can effectively solve path planning problems in multi-objective optimization.

Table 4. The path planning is according to the statistical table.

Method	Optimal solution	Path length	Smoothness	Running time/s
Hybrid genetic algorithm	89.63	193.63	11.365	2.639
Ours	87.22	173.99	13.569	1.732

In summary, the plant layout planning model and path planning model constructed in this paper can achieve reasonable design and optimal path planning design for the plant landscape space of Z Park.

5. Conclusion

This paper presents a digital plant landscape planning system based on a topological optimization algorithm. The system enables plant layout planning and achieves garden path optimization based on an improved artificial fish school algorithm. Taking Z Park as an example, the system achieves reasonable planning of plant layout in the park based on the layout characteristics of landscape spatial elements and the constructed plant layout planning model. The model yields maximum values for landscape connectivity, minimum values for ecological damage, and maximum values for spatial utilization of 5091, 1.089, and 0.228, respectively, all of which outperform the target values of the actual plan. The path planning method based on the improved artificial fish school algorithm reduces runtime by 34.4% compared to the hybrid genetic algorithm, and its optimal solution, path length, and smoothness all outperform the hybrid genetic algorithm. Test results in a simulation environment and actual case applications validate the feasibility and effectiveness of the system proposed in this paper.

Funding

This research was supported by the Scientific Research Basic Ability Improvement Project for Young and Middle-aged Teachers in Guangxi Universities In 2024: Research on the Relevance between the Biological Diversity of Landscape Plants and Landscape Design (2024KY0258).

References

1. Galán-Acedo, C., Arroyo-Rodríguez, V., Cudney-Valenzuela, S. J., & Fahrig, L. (2019). A global assessment of primate responses to landscape structure. *Biological Reviews*, 94(5), 1605-1618.
2. Landis, D. A. (2017). Designing agricultural landscapes for biodiversity-based ecosystem services. *Basic and Applied Ecology*, 18, 1-12.
3. Ai, J., & Kim, M. (2025). Research on Plant Landscape Design of Urban Industrial Site Green Space Based on Green Infrastructure Concept. *Plants*, 14(5), 747.
4. Yılmaz, S., Özgüner, H., & Mumcu, S. (2018). An aesthetic approach to planting design in urban parks and greenspaces. *Landscape Research*, 43(7), 965-983.
5. Yeom, S. J., & Lee, J. (2019). Changes of Landscape Perception in Seoullo7017 with Different Planting Design, based on Landscape Simulation. *Journal of Environmental Science International*, 28(11), 951-958.
6. Zhang, W. (2022). Design of urban garden landscape visualization system based on GIS and remote sensing technology. *Computational Intelligence and Neuroscience*, 2022(1), 9592376.
7. Chen, C., Wang, R., Chen, M., Zhao, J., Li, H., Ignatieva, M., & Zhou, W. (2025). The post-effects of landscape practices on spontaneous plants in urban parks. *Urban Forestry & Urban Greening*, 107, 128744.
8. Feng, L., & Zhao, J. (2021). Research on the construction of intelligent management platform of garden landscape environment system based on remote sensing images. *Arabian Journal of Geosciences*, 14, 1-19.
9. Lovett, A., Appleton, K., Warren-Kretzschmar, B., & Von Haaren, C. (2015). Using 3D visualization methods in landscape planning: An evaluation of options and practical issues. *Landscape and Urban Planning*, 142, 85-94.
10. Dong, J., Zhou, T., Xin, L., Tan, Y., & Wang, Z. (2018, February). The sustainable expression of ecological concept in the urban landscape environment design. In IOP conference series: Earth and environmental science (Vol. 113, No. 1, p. 012010). IOP Publishing.
11. Sun, S., Xu, X., Lao, Z., Liu, W., Li, Z., García, E. H., ... & Zhu, J. (2017). Evaluating the impact of urban green space and landscape design parameters on thermal comfort in hot summer by numerical simulation. *Building and Environment*, 123, 277-288.

12. Okasha, A. S., & Mekkawy, A. A. E. (2021). Participatory eco-landscape design: the case of NRIAG eco-park in Helwan, Egypt. *Journal of Engineering and Applied Science*, 68(1), 12.
13. Zheng, Y., Han, Q., & Keeffe, G. (2024). An evaluation of different landscape design scenarios to improve outdoor thermal comfort in Shenzhen. *Land*, 13(1), 65.
14. Lin, Z., Wang, Y., Song, Y., Huang, T., Gan, F., & Ye, X. (2022). Research on ecological landscape design and healing effect based on 3D roaming technology. *International journal of environmental research and public health*, 19(18), 11406.
15. Song, Y., & Jing, Y. (2020). Application prospect of CAD-SketchUp-PS integrated software technology in landscape planning and design. *Computer-Aided Design and Applications,* 18(S3), 153-163.
16. Deng, Y., Xie, L., Xing, C., & Cai, L. (2022). Digital city landscape planning and design based on spatial information technology. *Neural Computing and Applications*, 34(12), 9429-9440.
17. Pei, L. (2021). Green urban garden landscape design and user experience based on virtual reality technology and embedded network. *Environmental Technology & Innovation*, 24, 101738.
18. Lin, X., Song, J., An, M., & Li, Z. (2024). The Application of Computer Augmented Reality Technology to Landscape Design. *Procedia Computer Science*, 243, 187-196.
19. Yang, D., & Huang, X. (2024). Landscape design and planning methods for plant protection based on deep learning and remote sensing techniques. *Crop Protection*, 180, 106620.
20. Huang, L. (2021, April). Application of big data in improving landscape plant landscaping method. In Journal of Physics: Conference Series (Vol. 1852, No. 3, p. 032024). IOP Publishing.
21. Du, J. (2022). Application of CAD aided intelligent technology in landscape design. International *Journal of Advanced Computer Science and Applications*, 13(12).
22. Yang Zhang,Li Jiacheng & Li Lei. (2020). Time-Dependent Theme Park Routing Problem by Partheno-Genetic Algorithm. *Mathematics*,8(12),2193-2193.
23. Liu Yi,Feng Xuesong,Yang Yan,Ruan Zejing,Zhang Lukai & Li Kemeng. (2022). Solving urban electric transit network problem by integrating Pareto artificial fish swarm algorithm and genetic algorithm. *Journal of Intelligent Transportation Systems*,26(3),253-268.
24. Ho Min Lee,Ali Sadollah,Young Hwan Choi,Jin Gul Joo & Do Guen Yoo. (2024). Development and Sensitivity Analysis of an Improved Harmony Search Algorithm with a Multiple Memory Structure for Large-Scale Optimization Problems in Water Distribution Networks. *Sustainability*, 16(15), 6689-6689.